TOWARDS THE COMPREHENSION OF THE STACKING FAULT ENERGY IN Fe-Mn-Al-C STEELS

O. A. ZAMBRANO[1,2], J. A. CASTAÑEDA[1,3] AND M. CAMARGO[4]

[1] Research Group on Fatigue and Surfaces (GIFS), Mechanical Engineering School,
Universidad del Valle - Campus Meléndez
Calle 13 No. 100-00, 760034 Cali, Colombia
jaime.castaneda@correounivalle.edu.co

[2] Research Group on Tribology, Polymers, Powder Metallurgy and Processing of Solid Waste
(TPMR), Materials Engineering School, Universidad del Valle - Campus Meléndez
Calle 13 No. 100-00, 760034 Cali, Colombia
oscar.zambrano@correounivalle.edu.co

[3] Research on Energy and Materials (REM), Mechanical Engineering Faculty, Universidad
Antonio Nariño - Campus Farallones
Km 18 vía Cali-Jamundí, 760030 Cali, Colombia
jaimecastaneda@uan.edu.co

[4] Complex Systems Group - CICBA, Universidad Antonio Nariño - Campus Farallones
Km 18 vía Cali-Jamundí, 760030 Cali, Colombia
manuel.camargo@uan.edu.co

Key words: Stacking fault energy (SFE), deformation mechanisms, molecular dynamics (MD), Fe-Mn-Al-C steels, GSFE

Abstract. High manganese steels have been extensively studied in recent decades thanks to their astonishing mechanical properties. In particular, high manganese Fe-Mn-Al-C alloys feature an excellent combination of strength and ductility, properties that depend on the main deformation mechanism and therefore are determined by the stacking fault energy (SFE). To achieve a better understanding of the deformation mechanisms in this system, it is appealing to study the effect of the chemical composition as well as of temperature on the SFE from a microscopic perspective, which allows covering the most important features involved in this phenomenon. Recently, some insights regarding the TWIP phenomenon has been obtained by means of molecular dynamics simulations for a particular composition. In this work, we performed molecular dynamics simulations to systematically analyze the effects of the chemical composition on the SFE of austenitic Fe-Mn alloys. Our simulations are based on MEAM interatomic interaction potentials which have been proved to accurately reproduce fundamental structural and thermodynamic properties of Fe-Mn and Fe-Al binary systems. The obtained energy-displacements curves (i.e., generalized stacking fault curves) provide rich and useful information to comprehend the deformation mechanisms as well as being adopted in the classical thermodynamic

treatment of the SFE, and therefore they define an important starting step towards the comprehension of the behavior of the SFE for more complex Fe-Mn-Al-C alloys.

1 INTRODUCTION

The high manganese steels have gained significant attention over the recent years due to their exceptional combination of mechanical properties and low density, which make them very promising for many industrial applications. The uniqueness combination of high strength and high ductility of these steels relies on special deformation mechanisms such as transformation-induced plasticity (TRIP), twinning-induced plasticity (TWIP), microband-induced plasticity (MBIP) and dynamic slip band refinement (DSBR). The activation of these deformation mechanisms strongly depends on the stacking fault energy (SFE) of austenite [1, 2]. Moreover this metallurgical parameter has a high significance in several phenomena such as work hardening, fatigue, workability, wear, etc [3, 4, 5]. Nevertheless, it is known that the SFE *per se* could not be enough to describe the full relationship among the aforementioned phenomena and the deformation mechanisms in metals, being the main reason that the stacking faults as well as the nucleation of dislocations have a strong dependence of other parameters beyond the simple intrinsic SFE value. For this reason, the concept of the generalized stacking fault energy (GSFE) [6] is more adequate, since it has a deeper comprehension of the SFE.

The GSFE curve or γ-surface represents the energy cost per unite area by shifting two semi-infinite block of a crystal trough the (111) plane along $\langle 112 \rangle$ direction by a Burgers vector of a Shockley partial $\mathbf{b}_1$, i.e. $(\boldsymbol{a}/6)\langle 112 \rangle$, where a is the lattice parameter. The GSFE curve is full described by several parameters such as the unstable stacking fault energy γ_{USF}, the stacking fault γ_{SF} (also known as intrinsic stacking fault energy), and the unstable twin fault energy γ_{UTF}. These parameters are related to the nucleation of partial dislocations, the formation of stacking faults, and the formation of twin boundaries or also related to the "twinning tendency", among others. Nonetheless, studies of the γ-surface for binary, ternary o quaternary systems have been seldom addressed in the literature. In this sense, the present authors are making an effort to initiate the development of the first γ-surface for the Fe-Mn-Al-C system.

2 SIMULATION METHOD

We performed molecular dynamics simulations by using LAMMPS [7]. The modified embedded atom method (MEAM) [8, 9] was employed to evaluated the interactions between atoms. The energy in MEAM consists of two parts: a pair potential term specified by the function $\Phi(r)$ representing the electrostatic core-core repulsion, and a cohesive term specified by the function $F(\bar{\rho})$ representing the energy the ion core gets when it is embedded in the electron sea, i.e.

$$E_{\text{total}} = \sum_i \left[F_i(\bar{\rho}_i) + \frac{1}{2} \sum_{j \neq i} \Phi_{ij}(r_{ij}) \right] \tag{1}$$

The embedding energy is a function of the background electron density, which in turn is constructed as a superposition of contributions from neighbouring atoms. In this work, we considered the interatomic potentials for the $Fe_{1-x}Mn_x$ binary system to be these derived from the 2NN-MEAM formalism as explained in detail in [9].

Three dimensional fcc iron crystals were created within a simulation box which was oriented in such a way that its X, Y and Z axis were aligned with $[112]$, $[\bar{1}10]$, and $[\bar{1}\bar{1}1]$ crystal directions, respectively. Periodic boundary conditions were applied in X and Y directions while in the Z direction it was free. The initial box sizes were $L_X = 123.841$ Å, $L_Y = 102.142$ Å and $L_Z = 125.098$ Å, so that it initially contained $N = 134400$ Fe atoms. For a given composition, a number fraction x of Fe atoms was randomly chosen and replaced by Mn atoms. To take into account the effect of the disorder of the Mn-atoms location on the studied parameters, twenty independent simulations were analyzed for each composition. The equilibrium parameters, i.e., lattice parameter and cohesive energy, were determined by finding the minimum of the curve $E_{\text{total}}(V_{\text{box}}; x)$, where E_{total} represents the total potential energy of the system and $V_{\text{box}} = L_X L_Y L_Z$. Following the procedure described in [10], to determine the GSF curve the simulation box was split in two blocks by a (111) plane: a mobile upper block and a fixed lower block. Then the GSF curve was determined by rigidly displacing the upper block on a (111) plane along the $[11\bar{2}]$ direction while fixing the lower block and calculating the potential energy change per unit area with respect to the initial configuration. The upper block was displaced in forty steps of magnitude $\Delta S_X = b_1/20$ each; after each displacement step the system was allowed to relax in the Z-direction to attain the condition $P = 0$. To evaluate the surface energy, the upper block was vertically displaced a distance $\Delta S_Z = 2\,a$ and again the energy change was determined.

3 RESULTS

3.1 Lattice parameter, cohesive energy, and bulk modulus

In first place, the effect of the Mn content in the Fe-Mn system was studied through three well-known features: the lattice parameter a, the cohesive energy E_{coh}, and the bulk modulus B. For this analysis, the values obtained were normalized to the pure (fcc) iron values (see Table 1) as shown in Fig. 1. As can be seen in Fig. 1(a), the lattice parameter increase as the number of Mn atoms start to occupied or replace the Fe atoms in the fcc crystal structure by substitutional solid solution. This behavior is in perfect agreement with those found experimentally by X-ray diffraction in Fe-Mn-Al-C steels [11] and in the Fe-Mn system using *ab-initio* calculations [12, 13].

The cohesion energy, which is a measure of the forces that held the atoms together, is a parameter having important implications in properties such as elastic modulus, melting point, thermal expansion coefficient, etc. In this sense, the cohesion energy was calculate as a function of the Mn content as is shown in Fig. 1(b). For the best authors' knowledge, values of the cohesive energy for the Fe-Mn system are not available in the literature. Nevertheless, some estimations can be found for pure Mn and pure Fe elements, where the manganese has a lower cohesion energy than iron [14]. According to this, it seems
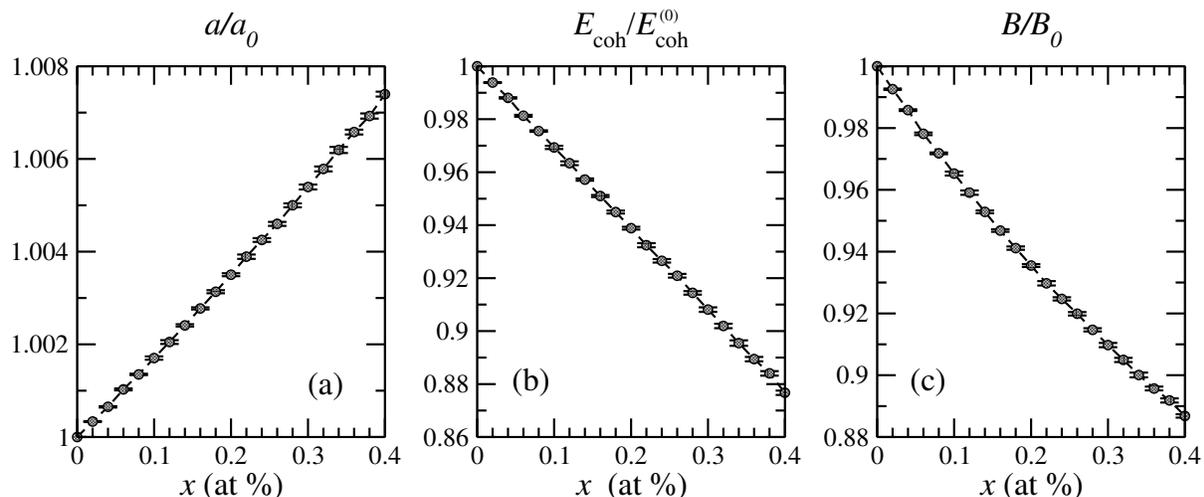
Figure 1: (a) Lattice parameter, (b) cohesive energy and (c) bulk modulus of austenitic $Fe_{1-x}Mn_x$ alloy system normalized to corresponding values of pure Fe (see Table 1).

Table 1: Lattice parameter, cohesive energy, bulk modulus, surface energy, and stacking fault energy calculated for pure (fcc) Fe at $T = 0$ K.

a_0 (Å)	$E_{coh}^{(0)}$ (eV)	B_0 (GPa)	$\gamma_{surf}^{(0)}$ (mJ/m^2)	$\gamma_{SF}^{(0)}$ (mJ/m^2)
3.6113	-4.2421	172.10	2087	-103.01

logical that as the manganese content increases in the Fe-Mn system, the cohesion energy should decrease; which is exactly the tendency observed in the present study.

Another valuable property is the bulk modulus B, which allow the prediction of some mechanical properties such as the fracture strength and resistance to plastic deformation in metals [15]. In fact, the ratio between B and the shear modulus G has been used to estimate the ductile or brittle behavior in metals [16]. In this regard, the effect of manganese on the bulk modulus in the Fe-Mn system was studied as shown in Fig. 1(c). There can be observed that as the manganese content increases B decreases linearly. This behavior is consistent with the experimental observations in the Fe-Mn system using nanoindentation, and also *ab-initio* calculations [17].

3.2 Surface energy

The surface energy is a property which has important implications in phenomena such as crystal growth, corrosion, and texture, etc. Together with the unstable stacking fault, the (111) surface energy γ_{surf} allows to determine the ductility parameter, which is a useful parameter for establishing the conditions for both brittle fracture and the nucleation and motion of dislocations. For this reason, the dependence of γ_{surf} on the Mn content was evaluated and the result is shown in Fig.2. The value of the surface energy for pure iron (fcc) in the (111) plane has a reported value of 1950 mJ/m^2 [18], and values between 2080 and 2100 mJ/m^2 using *ab-initio* calculations [19]. Thus, it can bee see in the present work, that for 0% Mn content, the surface energy is close to the values reported for pure

4
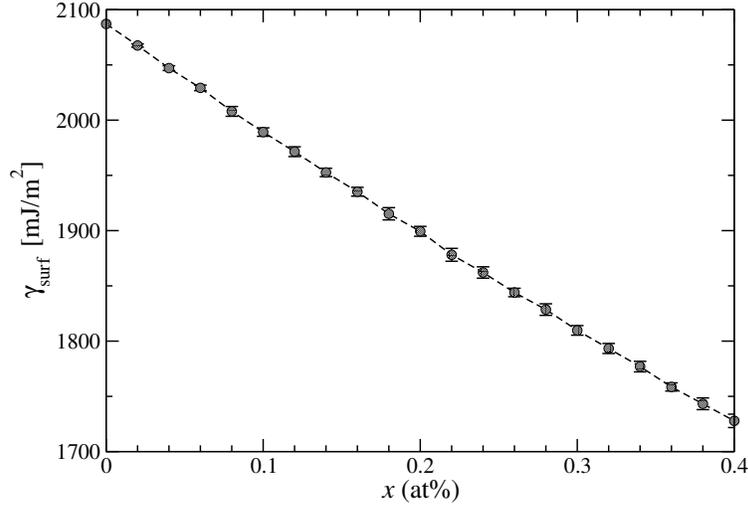
Figure 2: Surface energy of the $Fe_{1-x}Mn_x$ alloy system on the (111) plane

iron. In addition, it is known that the Mn has a lower surface energy than the Fe [20], and this effect can be seen as the addition of Mn atoms increase in Fe.

3.3   Generalized stacking fault energy (GSFE)

According to the previous calculations and analysis, it can be concluded that the employed interatomic potentials represent correctly the Fe-Mn system under the conditions evaluated. Then, the generalized stacking fault energy (GSFE) curve was constructed as function of the Mn content, as depicted in Fig. 3(a). There can be observed that
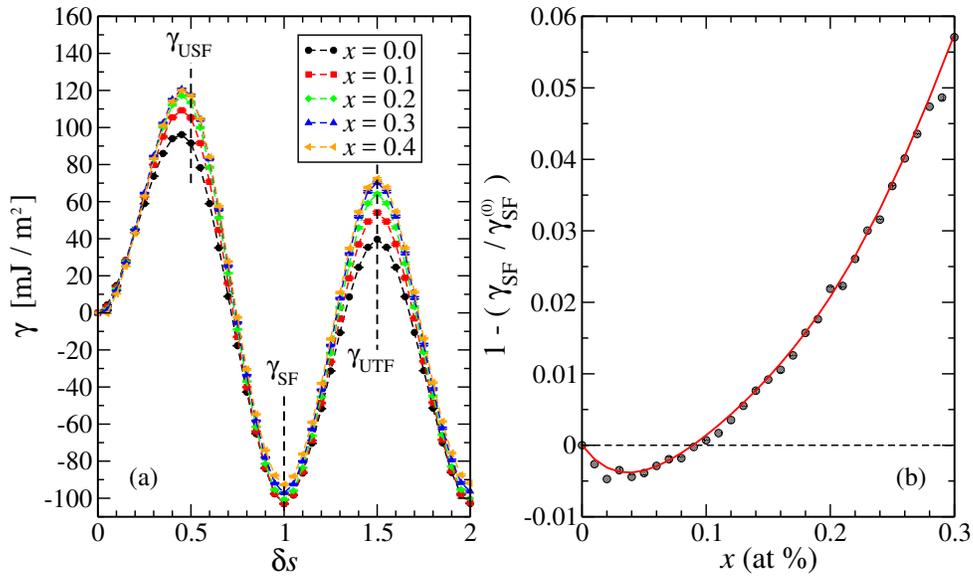
Figure 3: (a) GSE curves and (b) relative stacking fault energy for $Fe_{1-x}Mn_x$ alloy system ($T = 0$ K). In panel (a) $\delta s = \Delta S_X / b_1$ and the continuous line in panel (b) is a guide to the eye.

5

increasing the manganese content leads to larger values of both γ_{USF} and γ_{UTF} in a proportional way. However, the value of γ_{SF} decreases slightly with the manganese content. Figure 3(b) displays the (intrinsic) stacking fault energy normalized to corresponding value for pure iron. It can be observed that the SFE for $Fe_{1-x}Mn_x$ is smaller than that of pure iron up to $x = 10\%$ and the curve displays a parabolic behavior in this composition range. This behavior has been reported to occur with the addition of Mn in Fe-Mn [21] and Fe-Mn-Al-C [1] systems.

For a easy reading and interpretation, Fig. 4(a) presents γ_{USF}, γ_{SF}, and γ_{UTF} as a function of the manganese content. It is observed that the decrease or increase of these parameters does not obey a linear relation. Is important to point out that in the evaluated manganese range, we did not observe drastic changes of aforementioned parameters. Nevertheless, is possible that further increase of the Mn content changes the dependence observed, in other words, a plateau could occur (additional research is required in this direction). On the other hand, the nucleation of twins, i.e. the precursor of deformation twinning in fcc, has been showed to be intimately related to the γ_{UTF} [22] in the same manner as the γ_{SF} has been related to the emission of partial dislocations or the nucleation of perfect dislocations [6].
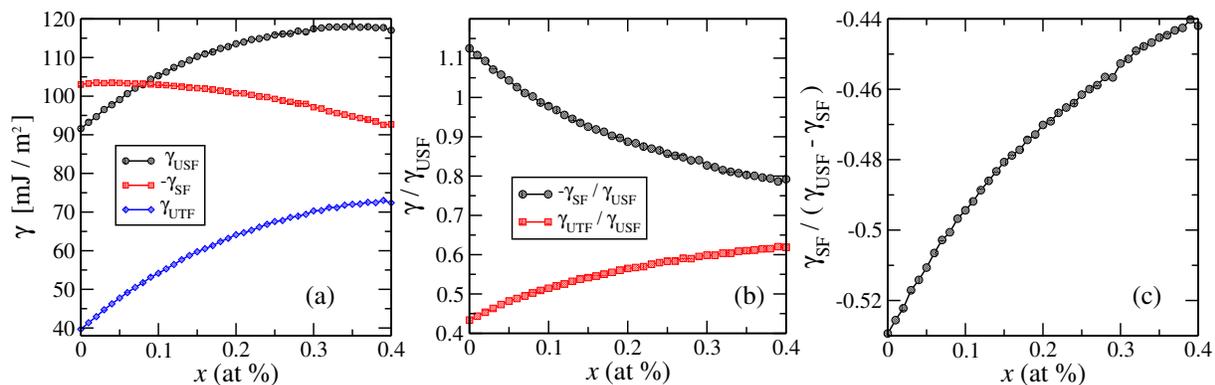
Figure 4: Unstable stacking fault energy γ_{USF}, intrinsic stacking fault energy γ_{SF}, unstable twinning energy γ_{UTF}, and relationships among them as functions of the Mn content for the $Fe_{1-x}Mn_x$ alloy system.

As can be seen in Fig. 4(b), as the Mn content increases the ratio $\gamma_{\text{SF}}/\gamma_{\text{USF}}$ decreases implying that the trailing partial dislocations nucleate with more difficulty, meaning in turn that the separation between the leading and trailing partials becomes broader, i.e. a change from full dislocation nucleation (unity) to a extended dislocation mechanism would occur. In addition, as the Mn content increases the ratio $\gamma_{\text{UTF}}/\gamma_{\text{USF}}$, which describes the competition between the energy barrier for twinning nucleation and full dislocation nucleation, also increases. In other words, twin nucleation should be favored as the Mn content increases. This implies that mechanical twinning should be present as main deformation mechanism in the Fe-Mn system, which is known to occur in Fe-Mn TWIP steels. However, so far it is no clear which deformation mechanism should take place in the others, i.e., formation of stacking fault over twin formation or vice versa. Thus, the

parameter $\gamma_{\mathrm{SF}}/(\gamma_{\mathrm{USF}} - \gamma_{\mathrm{SF}})$ can be useful to understand the deformation modes in the Fe-Mn alloy system (see Fig. 4(c)). It is known that when this parameter is negative, the formation of stacking faults occurs, thus, favoring a phase transformation from fcc to hcp crystal structure [23], i.e., transformation induced plasticity effect (TRIP). Returning to the Fig. 4(c), it can be seen that in all the composition range studied, this parameter has a negative value. However, as the manganese fraction increases, this parameter becomes less negative, which indirectly suggests that this deformation mechanism will be less extend, and another deformation mechanism should be operative at larger Mn contents.

4   CONCLUSIONS

Molecular dynamics simulations of the Fe-Mn system were performed to analyze the lattice parameter, the cohesion and surface energies, and the generalized stacking fault energy curve. The major conclusions are summarized as follows:

- The values obtained for the lattice parameter, cohesion energy, bulk modulus, and surface energy of the Fe-Mn system as a function of the Mn content is in a very good agreement with the experimental results as well as with *ab-initio* calculations.

- The GSFE curve allowed to analyze the effect of the manganese content on the γ_{USF}, γ_{SF}, and γ_{UTF} parameters, which are important to predict the deformation mechanisms.

- The ratio $\gamma_{\mathrm{SF}}/(\gamma_{\mathrm{USF}} - \gamma_{\mathrm{SF}})$ allowed to suggest that the main deformation mechanism in the Fe-Mn alloy system is the creation of stacking faults, which implies, the phase transformation from fcc to hcp crystal structure.

- The results obtained in this work will allow to contribute in the comprehension of the Fe-Mn-Al-C system, and provide a basis for this research avenue.

REFERENCES

[1] Zambrano, O.A. Stacking fault energy maps of Fe-Mn-Al-C-Si steels: Effect of temperature, grain size, and variations in compositions. *J. Eng. Mater. Technol.* (2016) **138**:041010.

[2] Li, W., Lu, S., Hu, Q.M., Johansson, B., Kwon, S.K., Grehk, M., Johnsson, J.Y., and Vitos, L. Generalized stacking fault energy of γ-Fe. *Philos. Mag.* (2016) **96**:524–541.

[3] Zambrano, O.A. A general perspective of Fe-Mn-Al-C steels. *arXiv preprint* (2017) arXiv:1707.01920v2.

[4] Zambrano, O.A., Valdés, J., Aguilar, Y., Coronado, J.J, Rodríguez, S.A., and Logé, R.E. Hot deformation of a Fe-Mn-Al-C steel susceptible of κ-carbide precipitation. *Mat. Sci. Eng. A.* (2017) **689**:269–285.

[5] Zambrano, O.A., Aguilar, Y., Valdés, J., Rodríguez, S.A., and Coronado, J.J. Effect of normal load on abrasive wear resistance and wear micromechanisms in FeMnAlC alloy and other austenitic steels. *Wear* (2016) **348–349**:61–68.

[6] Rice, J.R. Dislocation nucleation from a crack tip: An analysis based on the Peierls concept. *J. Mech. Phys. Solids* (1992) **40**:239–271.

[7] Plimpton, S. Fast parallel algorithms for short-range molecular dynamics. *J. Comp. Phys.* (1995) **117**:1–19.

[8] Baskes, M. Modified embedded-atom potentials for cubic materials and impurities. *Phys. Rev. B* (1992) **46**:2727–2742.

[9] Kim, Y.M., Shin, Y.H., and Lee, B.J. Modified embedded-atom method interatomic potentials for pure Mn and the FeMn system. *Acta Mater.* (2009) **57**:474–482.

[10] Zhang, L., Cheng, L., Kiet, T., Zhao, X., Pei, L.Q., and Guillaume, M. Molecular dynamics simulation on generalized stacking fault energies of fcc metals under preloading stress. *Chin. Phys. B* (2015) **24**:088106.

[11] Chu, C.M., Huang, H. Kao, P.W., and Gan, D. Effect of alloying chemistry on the lattice constant of austenitic Fe-Mn-Al-C alloys. *Scri. Metall. Mater.* (1994) **30**:505–508.

[12] Gebhardt, T., Music, D., Hallstedt, B., Ekholm, M., Abrikosov, I.A., Vitos, L., and Schneider, J. Ab initio lattice stability of fcc and hcp Fe-Mn random alloys. *J. Phys.: Condens. Matter* (2010) **22**:295402.

[13] Zhang, H., Punkkinen, M.P., Johansson, B., and Vitos, L. Elastic parameters of paramagnetic iron-based alloys from first-principles calculations. *Phys. Rev. B* (2012) **85**:054107.

[14] Turchanin, M. and Agraval, P. Cohesive energy, properties, and formation energy of transition metal alloys. *Powder Metall. Met. Ceram.* (2008) **47**:26–39.

[15] Pugh, S.F. XCII. Relations between the elastic moduli and the plastic properties of polycrystalline pure metals. *Lond. Edinb. Dubl. Phil. Mag.* (1954) **45**:823–843.

[16] Reeh, S., Music, D., Ekholm, M., Abrikosov, I.A., and Schneider, J.M. Elastic properties of fcc Fe-Mn-X (X = Cr, Co, Ni, Cu) alloys from first-principles calculations. *Phys. Rev. B* (2013) **87**:224103.

[17] Gebhardt, T., Music, D., Ekholm, M., Abrikosov, I.A., von Appen, J., Dronskowski, R., Wagner, D., Mayer, J., and Schneider, J.M. Influence of chemical composition and magnetic effects on the elastic properties of fcc Fe-Mn alloys. *Acta Mater.* (2011) **59**:1493–1501.

[18] Inman, M.C. and Tipler, H.R. Interfacial energy and composition in metals and alloys. *Metall. Rev.* (1963) **8**:105–166.

[19] Yu, J., Lin, X., Wang, J., Chen, J., and Huang, W. First-principles study of the relaxation and energy of bcc-Fe, fcc-Fe and AISI-304 stainless steel surfaces. *Appl. Surf. Sci.*, (2009) **255**:9032–9039.

[20] Lee, J.Y., Punkkinen, M.P.J., Schönecker, S., Nabi, Z., Kádas, K., Zólyomi, V., Koo, Hu, Q.M., Ahuja, R., Johansson, B., Kollár, J., Vitos, L., and Kwon, S.K. The surface energy and stress of metals. *Surf. Sci.* (2018) In Press.

[21] Lee Y.K. and Choi, C. Driving force for $\gamma - \epsilon$ martensitic transformation and stacking fault energy of γ in Fe-Mn binary system. *Metall. Mater. Trans. A* (2000) **31**:355–360.

[22] Tadmor E.B. and Hai, S. A Peierls criterion for the onset of deformation twinning at a crack tip. *J. Mech. Phys. Solids* (2003) **51**:765–793.

[23] Jo, M., Koo, Y.M., Lee, B.J., Johansson, B., Vitos, L., and Kwon, S.K. Theory for plasticity of face-centered cubic metals. *Proc. Natl. Acad. Sci.* (2014) **111**:6560–6565.